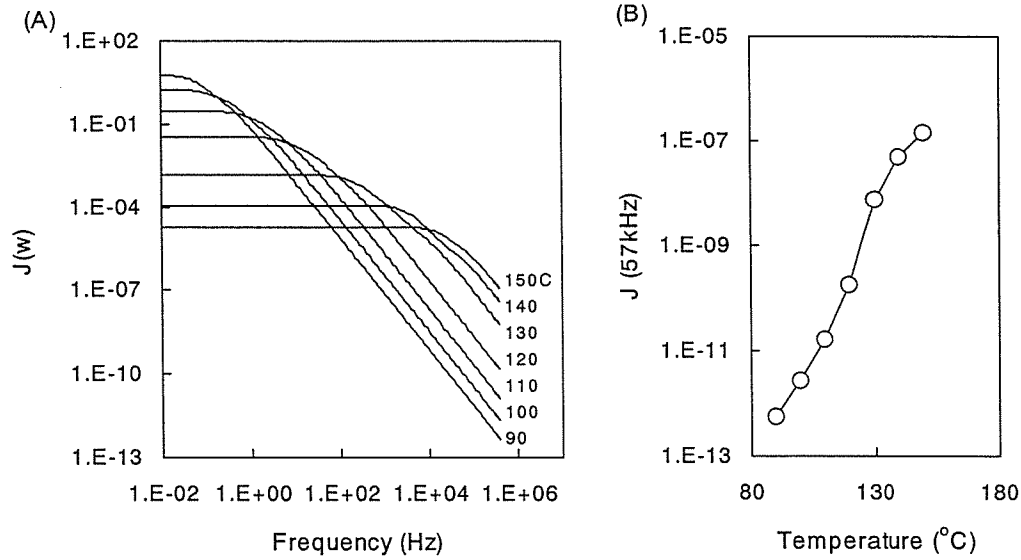

Fig.4. Spectral density calculated from dielectric relaxation spectrum of freeze-dried IMT as a function of frequency (A) and at 57 kHz as a function of temperature (B).

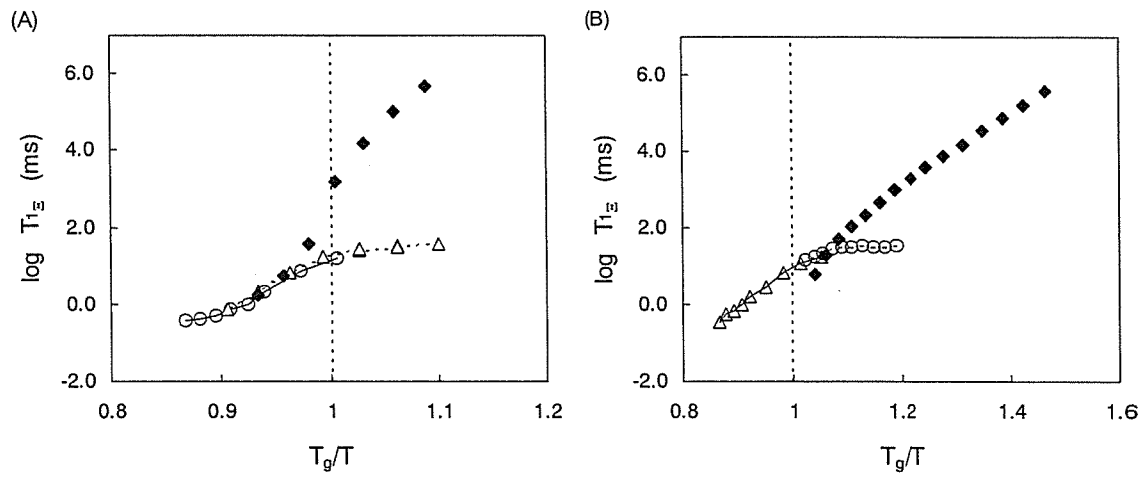

Fig.5. $T_{1\rho}$ observed at 43%RH (△) and 60%RH (○) for freeze-dried IMT (A) and that at 60%RH (○) and 75%RH (△) for freeze-dried dextran 40k (B), compared with $T_{1\rho}$ estimated based on the spectral density calculated from dielectric spectrum (◆).

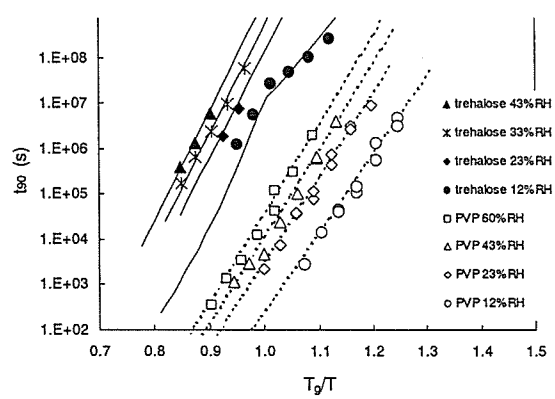

Fig.6. Temperature dependence of t_{90} for trehalose and PVP formulations

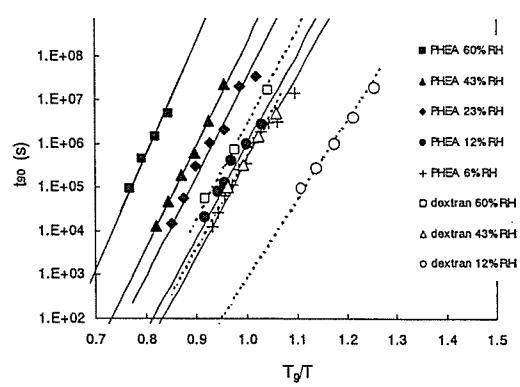

Fig.7. Temperature dependence of t_{90} for PHEA and dextran formulations

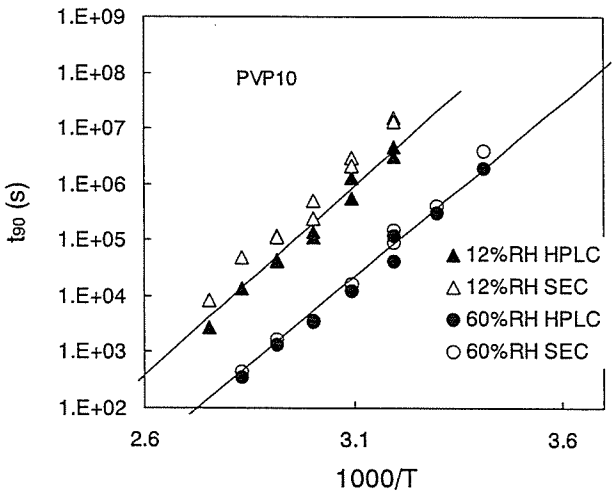

Fig.8. t_{90} for PVP formulation determined by HPLC and SEC

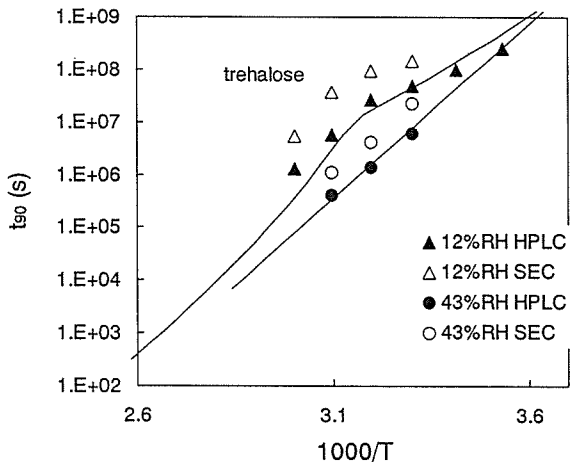

Fig.10. t_{90} for trehalose formulation determined by HPLC and SEC

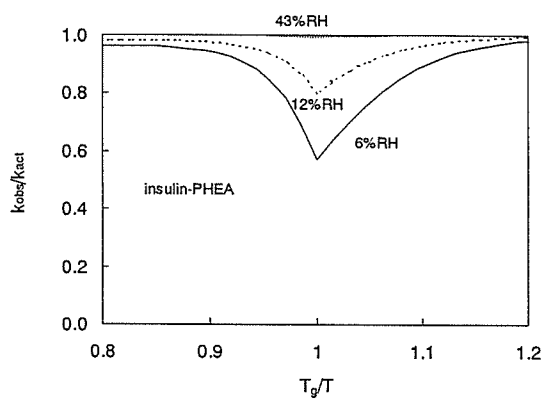

Fig.12. Degree of reduction in k_{obs} caused by reduced molecular mobility for PHEA formulation

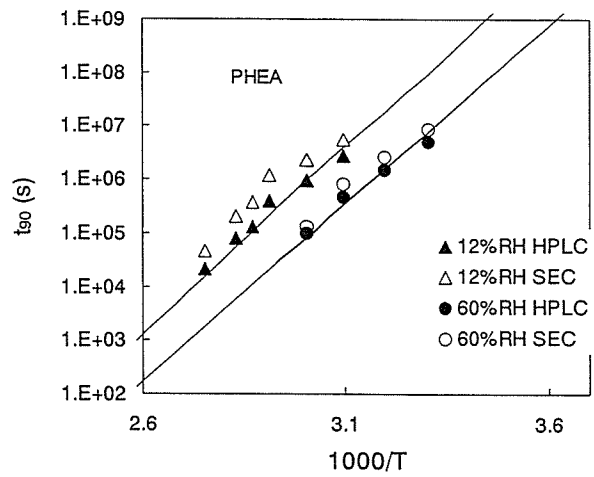

Fig.9. t_{90} for PHEA formulation determined by HPLC and SEC

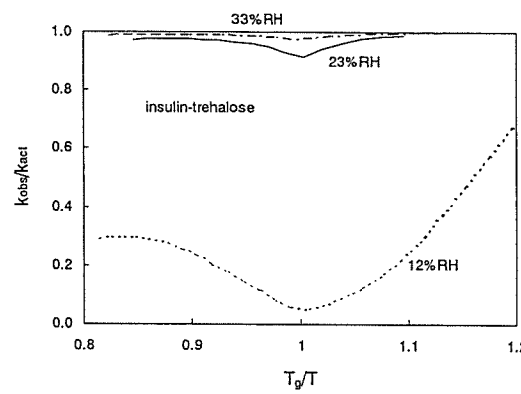

Fig.11. Degree of reduction in k_{obs} caused by reduced molecular mobility for trehalose formulation

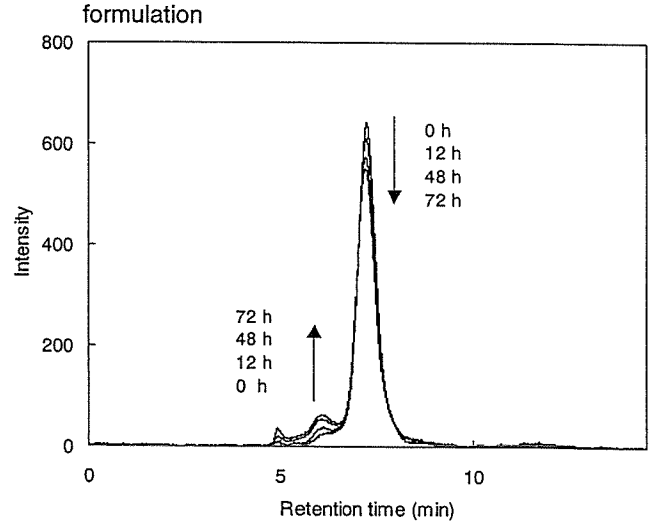

Fig.13. Size-exclusion chromatograms of β-GA lyophilized with trehalose after various periods of storage at 80°C and 12 %RH. The weight fraction of trehalose : 0.5.

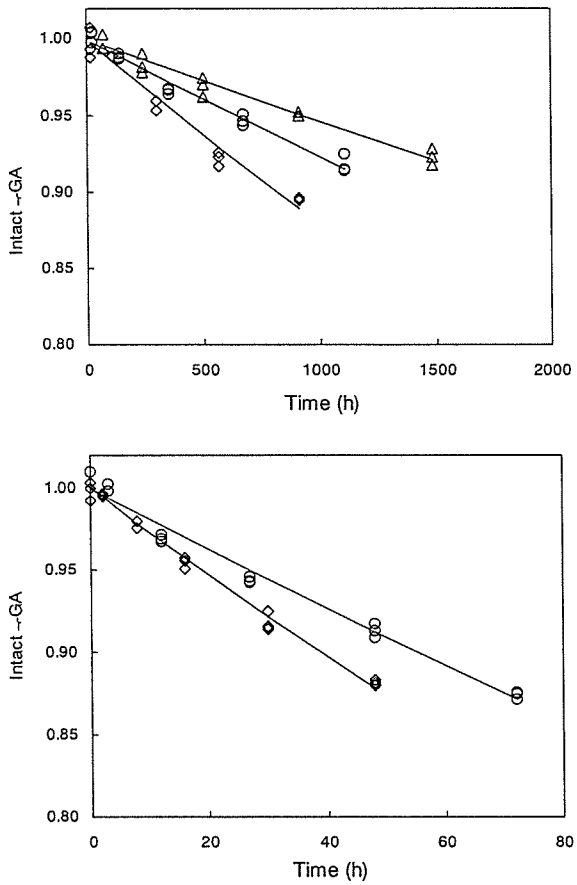

Fig.14. Time courses of aggregation of β-GA lyophilized with sucrose (△), trehalose (○) or stachyose (◇).
(A) aggregation at 50°C and excipient fraction of 0.33.
(B) aggregation at 80°C and excipient fraction of 0.5.

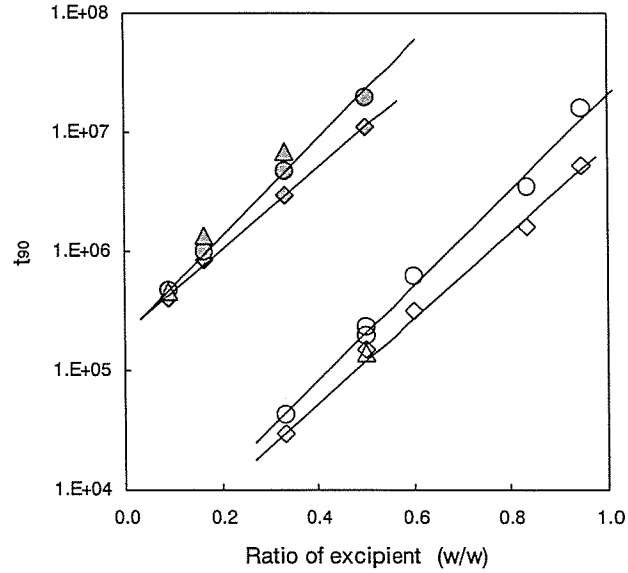

Fig.15. Dependence of t_{90} on the weight fraction of excipient. The value of t_{90} was determined at 80°C and 12 %RH for trehalose (○) and stachyose (◇), and at 50°C and 12 %RH for trehalose (●), sucrose (▲) and stachyose (◆).

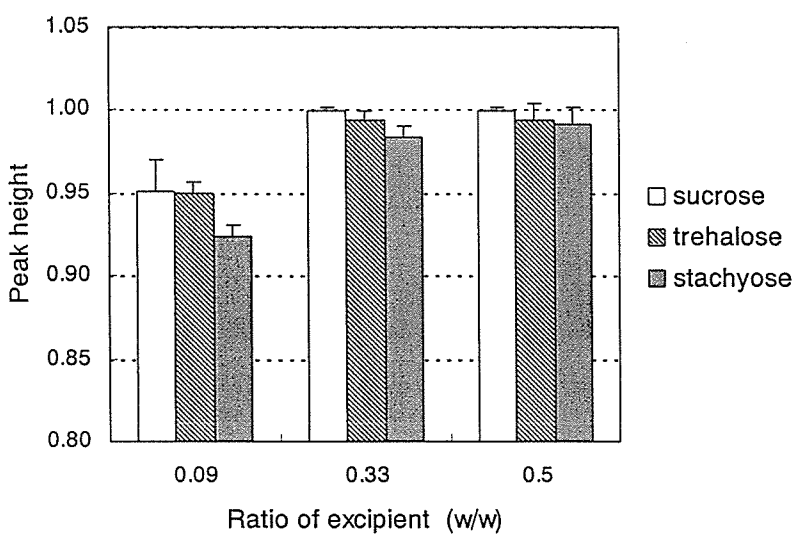

Fig.16. Effect of excipient fraction on aggregation of β-GA lyophilized with sucrose, trehalose or stachyose during freeze-drying process. Bars represent standard deviation (n=3).

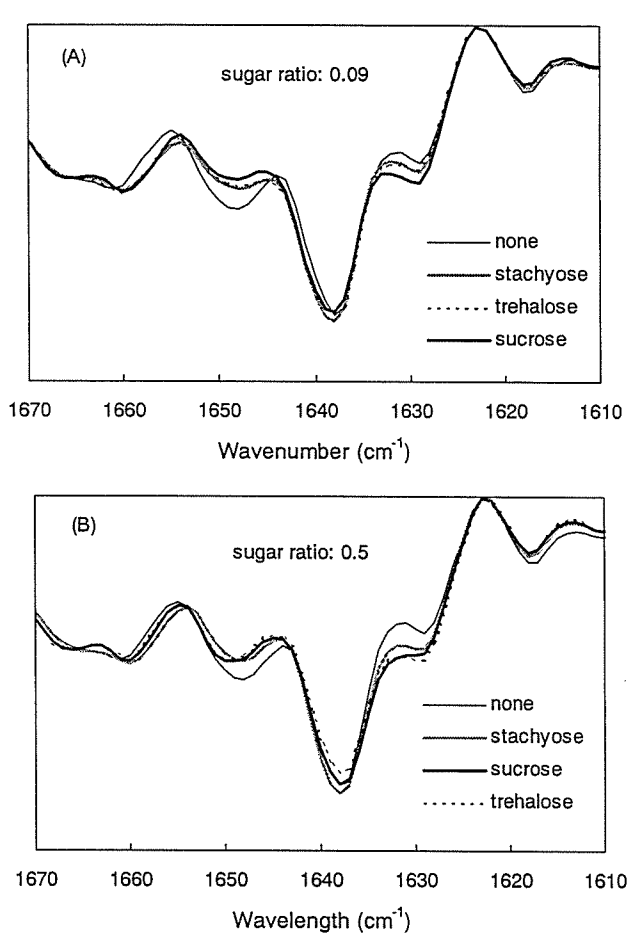

Fig.17. Second derivative FT-IR spectra for β-GA lyophilized with sucrose, trehalose or stachyose of 0.09 (A) and 0.5 fractions (B).

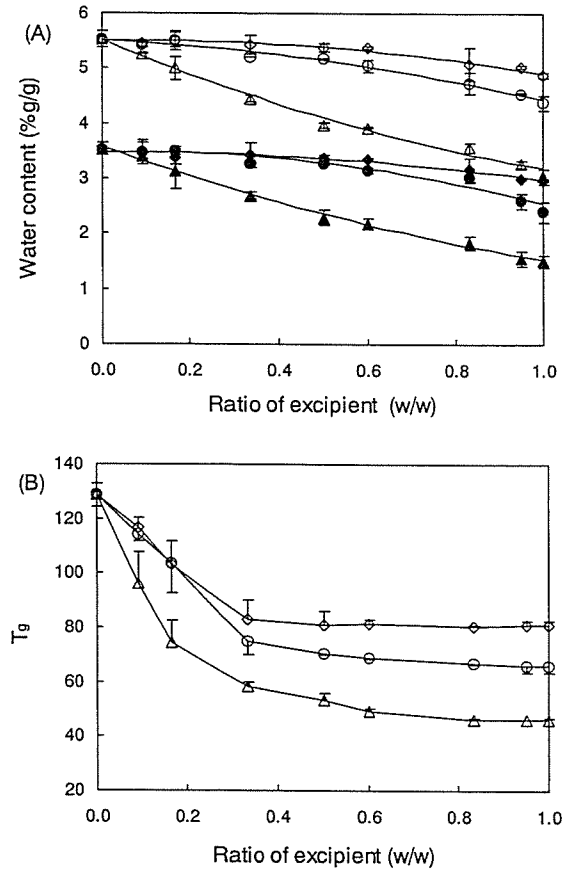

Fig.18. Water content (A) and Tg (B) of lyophilized β-GA formulations containing trehalose (○●), sucrose (△▲), or stachyose (◇◆) as a function of the weight fraction of excipient. (A) closed symbols: 10 %RH; open symbols: 20 %RH. 25°C. (B) 12 %RH. sd (n=3).

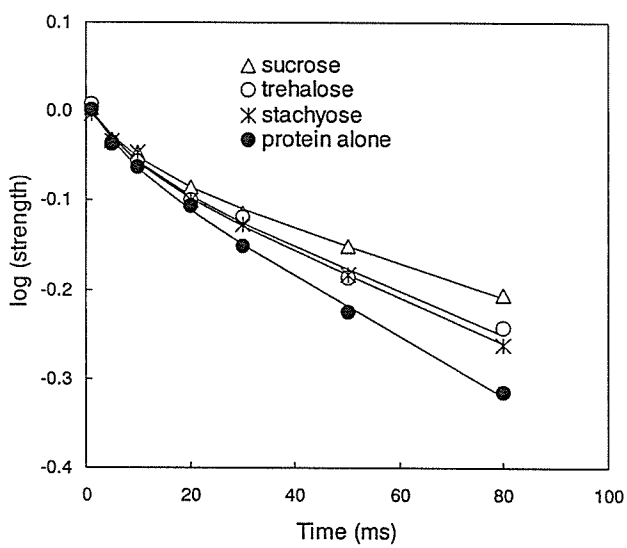

Fig.19. Time course of spin-lattice relaxation at 25°C and 12 %RH for carbonyl carbon of β-GA lyophilized with sucrose, trehalose or stachyose. The weight fraction of excipient : 0.5.

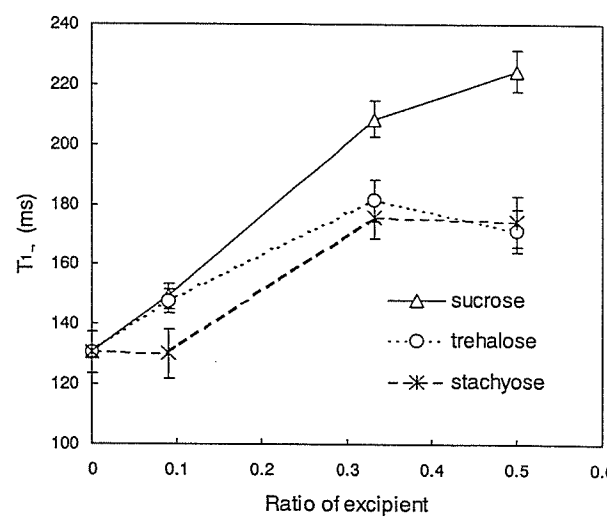

Fig. 20. Effect of weight fraction of excipient on $T_{1\rho}$ of carbonyl carbon at 25°C and 12 %RH for β-GA lyophilized with sucrose, trehalose or stachyose.

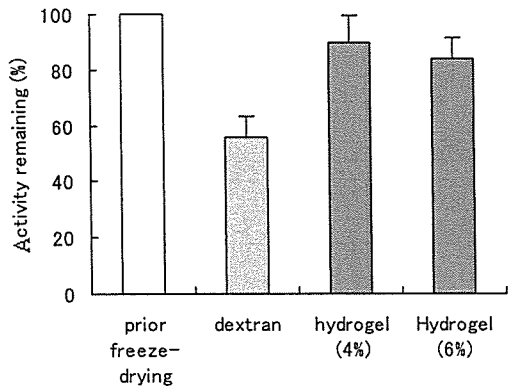

Fig.21. Effects of freeze-drying on β-galactosidase activity

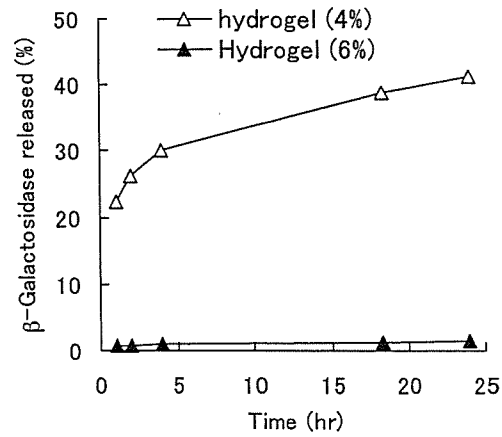

Fig.22. Release profiles of β-galactosidase from dextran hydrogel microspheres

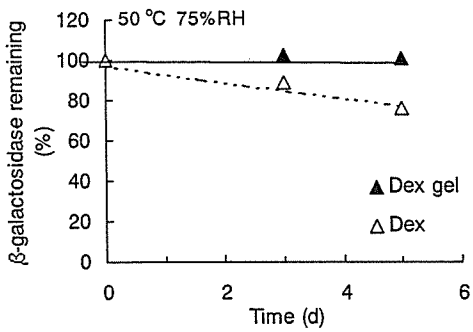

Fig. 23. Effect of storage on β-galactosidase activity in dextran gel

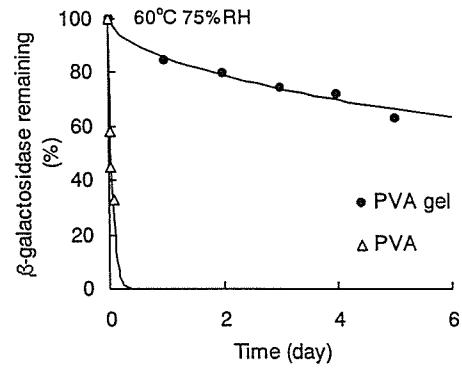

Fig. 24. Effect of storage on β-galactosidase activity in PVA gel

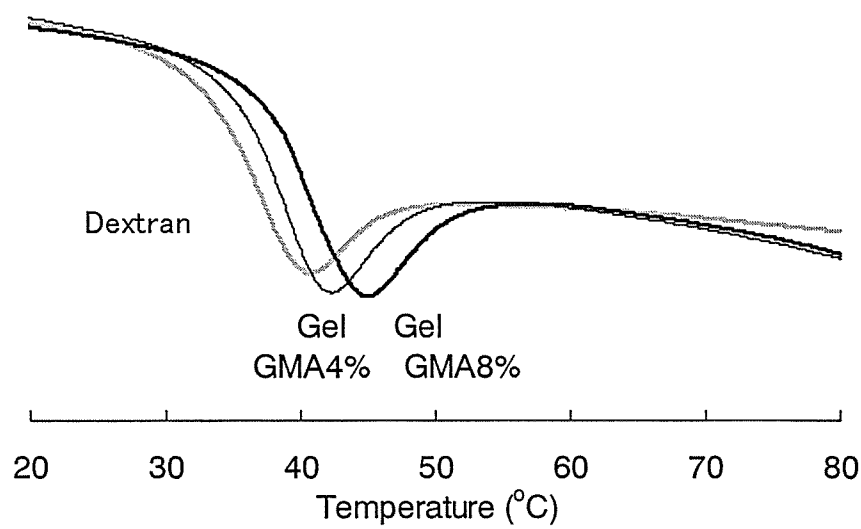

Fig. 25. Effect of cross-linking on T_g of dextran.
Water content of the sample was adjusted by storering at 25 °C and 75%RH for 1 day.

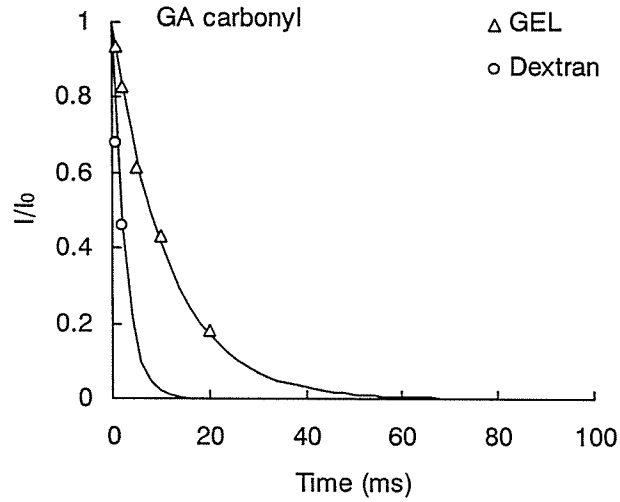

Fig. 26. Time corse of spin-lattice relaxation of β-galacosidase carbonyl carbons in dextran gels and freeze-dried dextran formulation.
Water content of the sample was adjusted by storering at 25 °C and 75%RH for 1 day.

<凍結乾燥再水和法 Dehydration Rehydration Vesicle (DRV法)>

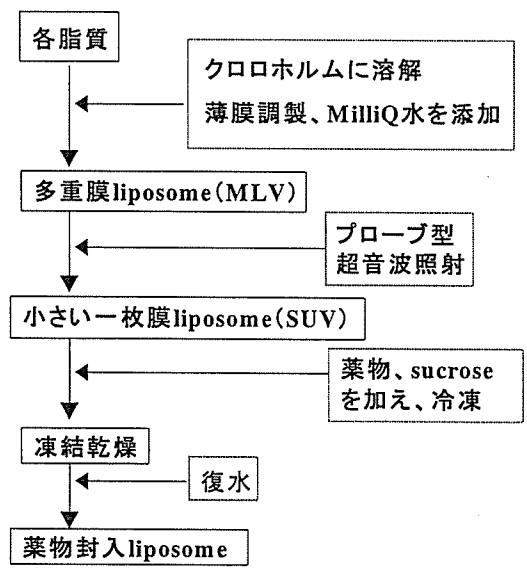

Fig.27. Preparation of Dehydration Rehydration Vesicle

凍結過程におけるショ糖の役割

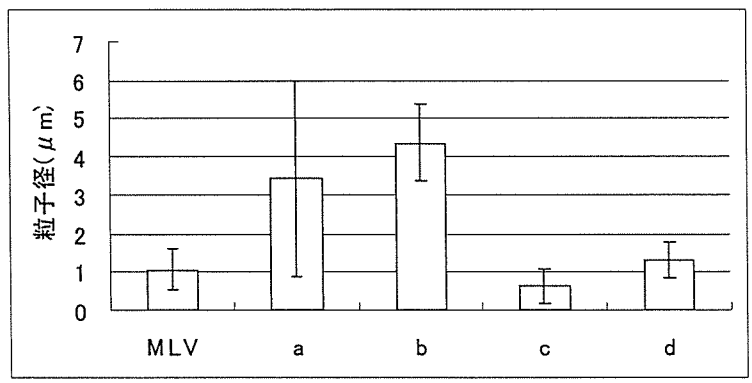

a) MLV　急速凍結　室温融解
b) MLV　凍結　室温融解
c) MLV ＋ショ糖　急速凍結　室温融解
d) MLV ＋ショ糖　凍結　室温融解

Fig.28. Effect of sucrose on particle size of liposome after freeing and thawing

凍結乾燥と再水和過程におけるショ糖の役割

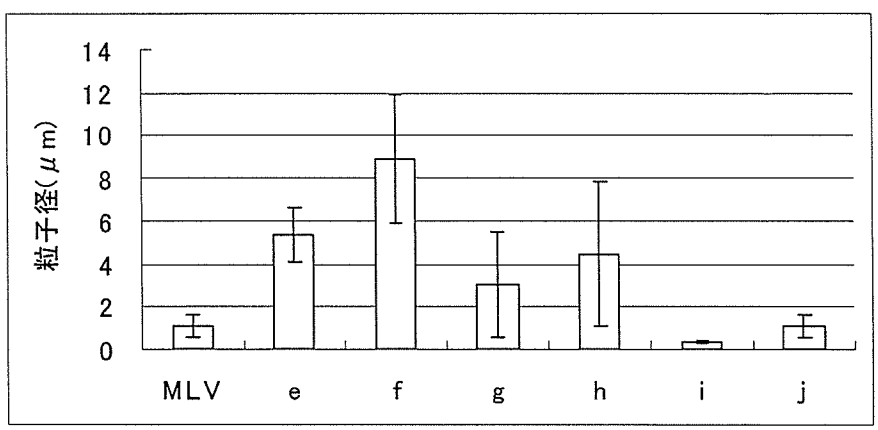

e) MLV　急速凍結乾燥　ショ糖再水和
f) MLV　凍結乾燥　ショ糖再水和
g) MLV　急速凍結乾燥　水再水和
h) MLV　凍結乾燥　水再水和
i) MLV ＋ショ糖　急速凍結乾燥　水再水和
j) MLV ＋ショ糖　凍結乾燥　水再水和

Fig.29. Effect of sucrose on particle size of liposome after freeze-drying and rehydration

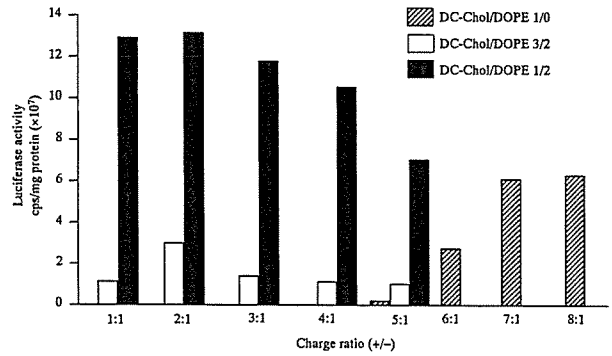

Fig.30. （+/−）荷電比を変えた時のリポソーム/DNA 複合体ベクターによる遺伝子導入効率

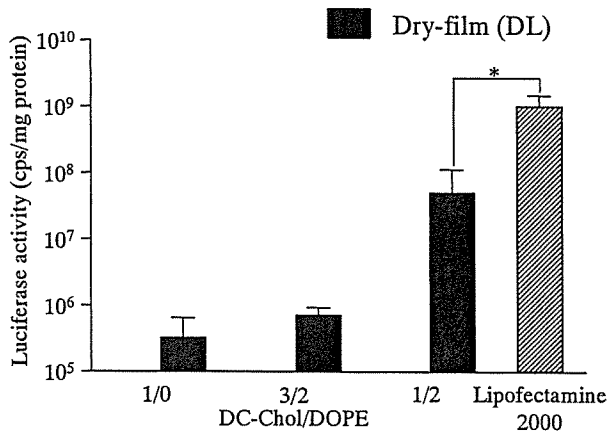

Fig.31. 最適混合荷電比 （+/−）でのリポソーム/DNA 複合体ベクターによる遺伝子導入効率

Table 1 遺伝子封入リポソーム製剤の組成

DC-Chol：DOPE(モル比)		DNA (μg)	糖	+/-
3:2	B-1	25	Sucrose	16:1
3:2	B-2	25	Isomaltose	16:1
3:2	B-3	25	Isomaltotriose	16:1
1:2	C-1	100	Sucrose	2:1
1:2	C-2	100	Isomaltose	2:1
1:2	C-3	100	Isomaltotriose	2:1
1:2	C-4	12.5	Sucrose	16:1
1:2	C-5	12.5	Isomaltose	16:1
1:2	C-6	12.5	Isomaltotriose	16:1

Table 2 遺伝子封入リポソーム製剤の再水和後の粒子サイズ

DC-Chol：DOPE(モル比)		平均サイズ(nm)	分散 (%)	平均サイズ(nm)	分散 (%)
3:2	B-1	179	62	1274	38
3:2	B-2	178	69	1269	31
3:2	B-3	191	70	1558	30
1:2	C-1	448	10	3495	90
1:2	C-2	364	8	3826	92
1:2	C-3	487	11	3161	88
1:2	C-4	238	30	1451	70
1:2	C-5	256	32	1591	68
1:2	C-6	205	32	1130	68

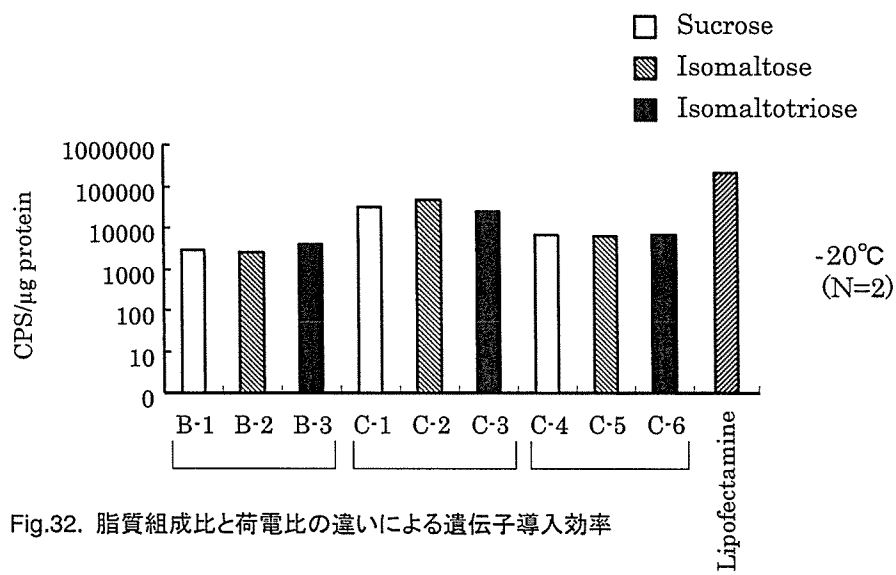

Fig.32. 脂質組成比と荷電比の違いによる遺伝子導入効率

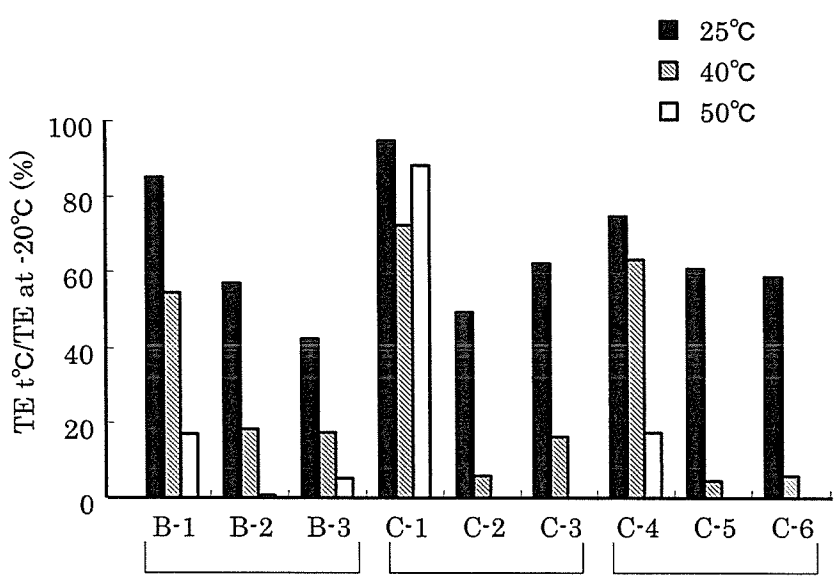

Fig.33. 保存温度によるルシフェラーゼ活性低下率

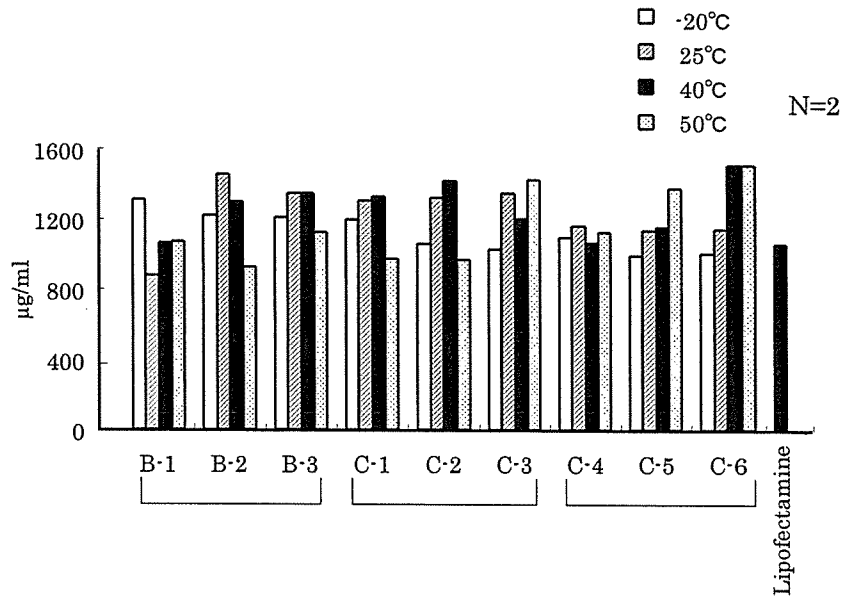

Fig.34. 遺伝子導入リポソーム製剤の細胞毒性

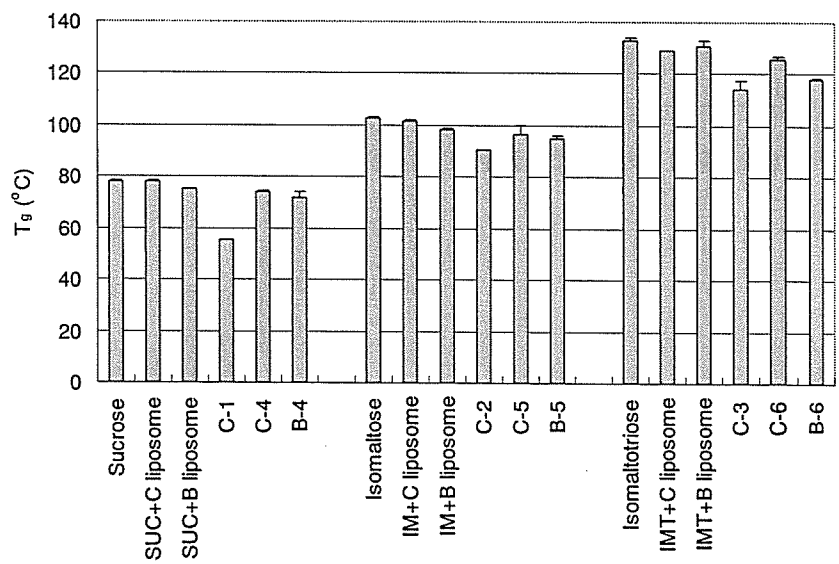

Fig. 35 T_g of Plasmid DNA-liposome formulations.

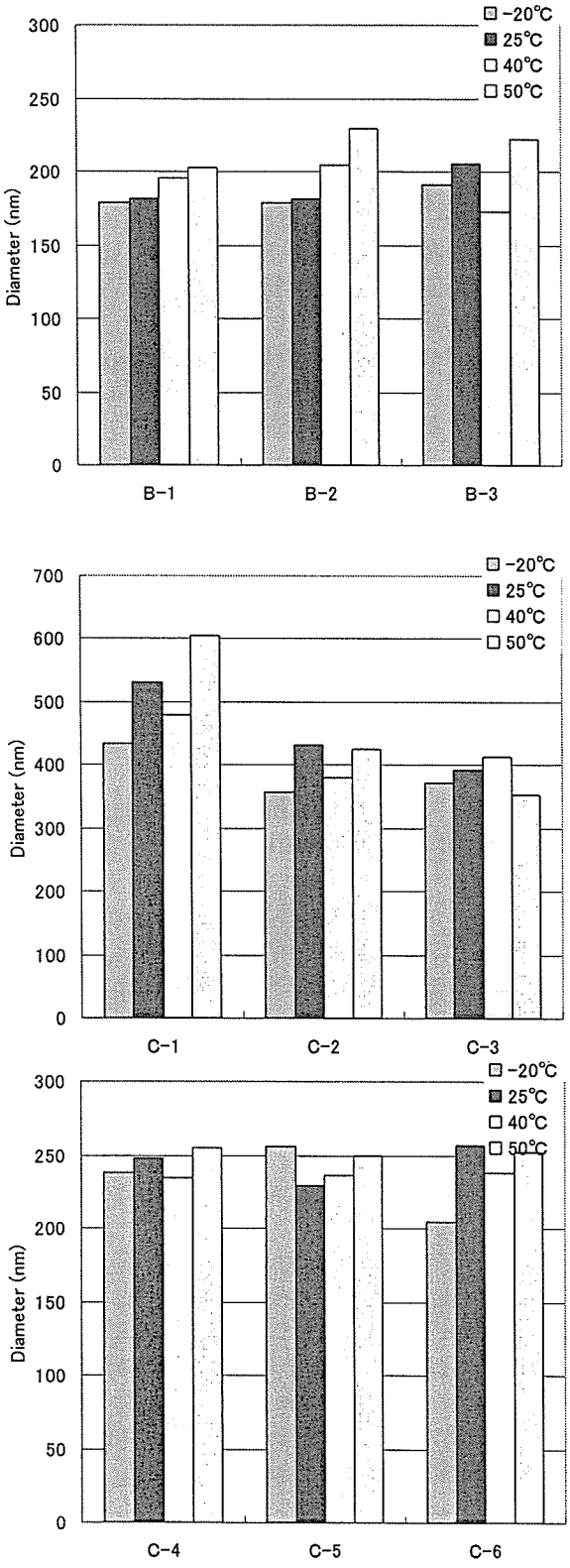

Fig.36 Particle size of lioposomes after rehydoration of lasmid DNA-liposome formulations stored at various temperature for 50 days.

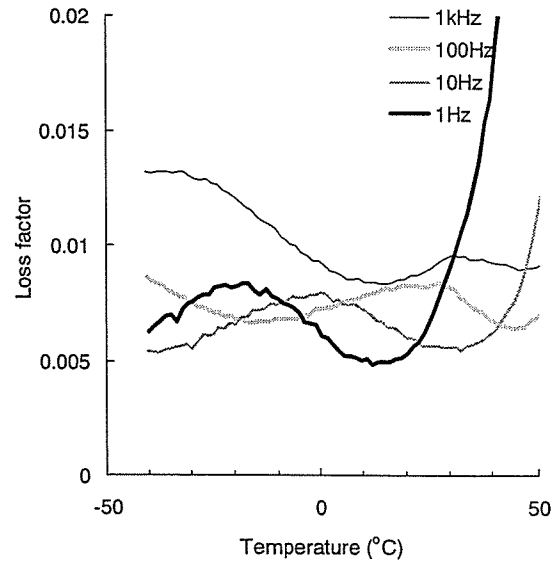

Fig.37. Temperature dependece of los facotr of freezed dried sucrose.

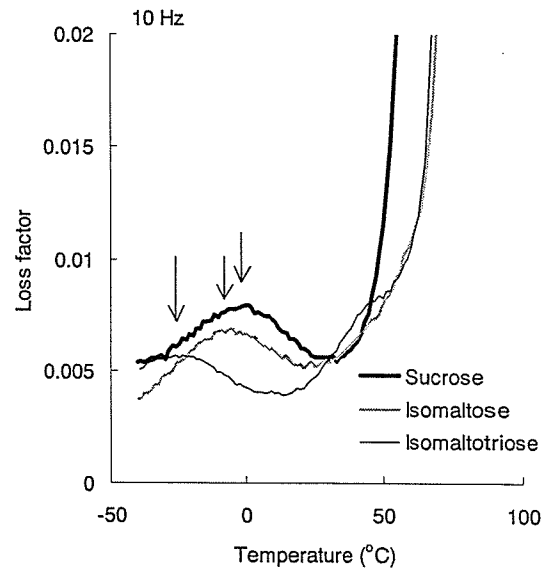

Fig.38 Temperature dependence of b-relaxation of freeze-dried sucrose, isomaltose and isomaltotriose.

研究成果の刊行に関する一覧表

雑誌

発表者氏名	論文タイトル名	発表誌名	巻名	ページ	出版年

1) T. Miyazaki, S. Yoshioka, Y. Aso, T. Kawanishi, Crystallization rate of amorphous nifedipine analogues unrelatd to the glass transition temperature. *Int. J. Pharm.* (2006) Accepted.
2) S.Yoshioka, Y.Aso, Correlations between Molecular Mobility and Chemical Stability during Storage of Amorphous Pharmaceuticals *J. Pharm. Sci.*, (2006) Accepted.
3) S.Yoshioka, T. Miyazaki, Y.Aso, Degradation Rate of Lyophilized Insulin, Exhibiting an Apparent Arrhenius Behavior around Glass Transition Temperature Regardless of Significant Contribution of Molecular Mobility. *J. Pharm. Sci.*, (2006) **95**, 2684-2691.
4) S.Yoshioka, T. Miyazaki, Y.Aso. β-relaxation of insulin molecule in lyophilized formulations containing trehalose or dextran as a determinant of chemical reacivity. *Pharm. Res.*, (2006) **23**, 961-966.
5) T. Miyazaki, S. Yoshioka, Y. Aso, Physical Stability of amorphous acetanilide derivatives imporoved by polymer excipients. *Chem. Pharm. Bull.*, (2006) 54, 1207-1210.
6) S.Yoshioka, Y.Aso, T. Miyazaki, Negligible contribution of molecular mobility to the degradation rate of insulin lyophilized with poly(vinylpyrrolidone). *J. Pharm. Sci.*, (2006) **95**, 939-943.
7) Y. Aso, S. Yoshioka, Molecular Mobility of Nifedipine-PVP and Phenobarbital-PVP Solid Dispersions as Measured by ^{13}C-NMR Spin-Lattice Relaxation Time. *J.Pharm.Sci.*, (2006) **95**, 318-325.
8) M. Fukushima, Y. Hattori, T. Yoshizawa, Y. Maitani. Combination of non-viral connexin 43 gene therapy and docetaxel inhibits the growth of human prostate cancer in mice. International Journal of Oncology, 30:225-231 (2007).
9) M. Watanabe, K. Kawano, M. Yokoyama, P. Opanasopit, T. Okano, Y. Maitani, Preparation of camptothecin-loaded polymeric micelles and evaluation of stability in vitro and in vivo, *Int. J. Pharm.*, 308:183-189(2006).
10) L. Feng, X. R. Qi, X. J. Zhou, Y. Maitani, S. C. Wang, Y. Jiang, T. Nagai, Pharmaceutical and immunological evaluation of a single-dose hepatitis B vaccine using PLGA microspheres, *J Control Release.* 112(1):35-42, (2006).
11) M. Furuhata, H. Kawakami, K. Toma, Y. Hattori, Y. Maitani, Design, synthesis and gene delivery efficiency of novel oligo-arginine linked PEG-lipids: effect of oligo-arginine length. *Int. J. Pharm.* 316(1-2): 109-116 (2006).
12) Y. Hiruta, Y. Hattori, K. Kawano, Y. Obata, Y. Maitani, Novel ultra-deformable vesicles entrapped with bleomycin and enhanced to penetrate rat skin, *J Control Release.*, 113: 146-154 (2006).
13) K. Kawano, M. Watanabe, T. Yamamoto, M. Yokoyama, P. Opanasopit, T. Okano, Y. Maitani, Enhanced antitumor effect of camptothecin loaded in long-circulating polymeric micelles, *J Control Release.*, 112: 329-332 (2006).
14) T. Yoshitomi, S. Yabuki, H. Kawakami, R. Sato, K. Toma, M. Furuhata and Y. Maitani, The structure of artificial lipids possessing oligo(ethylene glycol) and their behavior in water. *Colloids and Surfaces A.*, 284-285: 276-283, (2006).
15) S. Igarashi, Y. Hattori and Y. Maitani, Biosurfactant MEL-A enhances cellular association and gene transfection by cationic, *J Control Release.* 112: 362-368 (2006).
16) M. Furuhata, H. Kawakami, K. Toma, Y. Hattori, Y. Maitani, Intracellular delivery of proteins in complexes with oligoarginine -modified liposomes and the effect of oligoarginine length, *Bioconjugate Chemistry.*, 17: 935-942 (2006).
17) Y. Hattori and Y. Maitani, Two-step transcriptional amplification-lipid-based nanoparticles using PSMA or midkine promoter for suicide gene therapy in prostate cancer. Cancer Science. 97: 787-798 (2006).
18) K. Hayashi, JB Lee, Y. Maitani, N. Toyooka, H. Nemoto, T. Hayashi, The role of a HSV thymidine kinase stimulating substance, scopadulciol, in improving the efficacy of cancer gene therapy. *J Gene Med.* 8(8):1056-67 (2006).
19) Y. Maitani, S.Yano, Y. Hattori, M. Furuhata, Y.Hayashi, Liposome vector containing biosurfactant-complexed DNA as herpes simplex virus thymidine kinase gene delivery system. *J Lipsome Res.* 16:359-372 (2006).
20) S.Yoshioka, Y.Aso, Comparison of the glass transition temperature and fragility parameter of isom alto-olygomer predicted by molecular dynamics simulations with those measured by differential scann ing calorimetry. *Chem. Pharm. Bull.* 53:1443-1445 (2005).
21) S.Yoshioka, Y.Aso, A quantitative assessment of the significance of molecular mobility as a dete rminant for the stability of lyophilized insulin formulations. *Pharm. Res.* 22: 1358-1364 (2005)
22) Y. Aso, S. Yoshioka, Effect of Freezing Rate on Physical Stability of Lyophilized Cationic Lipos omes. *Chem. Pharm. Bull.*, 53, 301-304 (2005).

23) S.Yoshioka, Y.Aso, Glass transition- Related Changes in Molecular Mobility below Glass Transitio n Temperature of Freeze-dried Formulations, as Measured by Dielectric Spectroscopy and Solid State NMR. *J.Pharm. Sci.*, 94:275-287 (2005).
24) W.X. Ding, X.R. Qi, P. Li, Y. Maitani, T. Nagai, Cholesteryl hemisuccinate as a membrane stabiliz er in dipalmitoylphosphatidylcholine liposomes containing saikosaponin-d. *Int. J. Pharm.*, 300(1-2): 38-47, (2005).
25) P. Opanasopit, M. Yokoyama, M. Watanabe, K. Kawano, Y. Maitani, T. Okano, Influence of serum and albumins from different species on stability of camptothecin-loaded micelles. *J. Control. Release*, 104(2):313-21, (2005).
26) Y. Hattori, H. Kubo, K. Higashiyama and Y. Maitani, Folate-linked nanoparticles formed with DNA c omplexes in sodium chloride solution enhance transfection efficiency, *J. Biomedical Nanotechnology*, 1(2):176-184, (2005).
27) K. G. Lau, Y. Hattori, S. Chopra, E. A. O'Toole, A. Storey, T. Nagai and Y. Maitani, Ultra-deform able liposomes containing bleomycin: In vitro stability and toxicity on human cutaneous keratinocyt e cell lines, *Int. J. Pharm.*, 300:4-12, (2005).
28) Y. Hattori, and Y. Maitani, Folate-linked nanoparticle-mediated suicide gene therapy in human pro state cancer and nasopharyngeal cancer with herpes simplex virus thymidine kinase, *Cancer Gene Ther apy*, 12: 796-809, (2005).
29) Y. Hattori, and Y. Maitani, Folate-linked lipid-based nanoparticle for targeted gene delivery, *Cu rrent Drug Delivery*, 2:243-252, (2005).
30) J. Shi, W. Yan, X. Qi, Y. Maitani, and T. Nagai, Characteristics and biodistribution of soybean s terylglucoside and polyethylene glycol modified cationic liposomes and their complexes with antisen se oligodeoxynucleotide for hepatitis B virus therapy, *Drug Delivery*, 12(6):349-356, (2005).
31) T. Shiokawa, Y. Hattori, K. Kawano, Y. Ohguchi, H. Kawakami, K.Toma, and Y. Maitani, Effect of th e Polyethylene Glycol linker Chain Length of Folate-linked Microemulsions Loading Aclacinomycin A o n Targeting Ability and Antitumor Effect in vitro and in vivo, *Clinical Cancer Res*, 11(5):2018-25 (2005).
32) Y. Maitani, K. Nakamura, K. Kawano. Application of sterylglucoside-containing particles for drug delivery. *Curr. Pharm. Biotechnol*, 6, 81-93 (2005).
33) M. Furuhata, H. Kawakami, K. Toma, Y. Hattori and Y. Maitani, Design, Synthesis and Gene Delivery Efficiencies of Novel oligo-Arginine Linked PEG-Lipid: Effect of Oligo-Arginine Length, *Peptide Sc ience* 2004, 241-242, (2005).
34) T. Miyazaki, Y. Aso, S. Yoshioka, S. Kojima. Ability of polyvinylpyrrolidone and polyacrylic aci d to inhibit the crystallization of amorphous acetaminophen. *J. Pharm. Sci.*, 93: 2710-2717 (2004)
35) S.Yoshioka, Y.Aso, S.Kojima. Temperature- and glass transition temperature-dependence of bimolec ular reaction rates in lyophilized formulations described by Adam-Gibbs-Vogel equation, *J.Pharm. Sc i.*, 93, 1062-1069 (2004)
36) Y. Aso, S. Yoshioka, S. Kojima, Molecular mobility-based prediction of the crystallization rate o f amorphous nifedipine and phenobarbital in PVP solid dispersions. *J. Pharm. Sci.*, 93, 384-391 (200 4).
37) C. Xiao, X. Qi, Y. Maitani, and T. Nagai, Sustained-release of cisplatin from multivesicular lipo somes: potentiation of antitumour efficacy against S180 murine carcinoma, *J. Pharm. Sci.*, 93(7) 171 8-24 (2004).
38) T. Nagamoto, Y. Hattori, K. Takayama, and Y. Maitani, Novel chitosan particles and chitosan-coate d emulsions inducing immune response via intranasal vaccine delivery, *Pharm. Res.*, 21 (4): 671-674 (2004).
39)Y. Hattori and Y. Maitani, Enhanced in vitro DNA transfection *efficiency by novel folate-linked na noparticles in human prostate cancer and oral cancer, J.* Contr. Release, .79(1-3):147-55 (2004).
40) 米谷芳枝, 機能性脂質マイクロエマルションとDDS, 医薬ジャーナルMedical Front Line, 40, 37-43 (2004).
41)T. Fan, K. Takayama, Y. Hattori, and Y. Maitani, Formulation Optimization of Paclitaxel Carried by Pegylated Emulsions Based on Artificial Neural Network, *Pharm. Res.*, 21(9) 1694-1699 (2004).
42)M. Yokoyama, P.Opanasopit, T. Okano, Y. Maitani, and K. Kawano, Polymer design and incorporation m ethod for polymeric micelle carrier system containing water-insoluble anti-cancer agent camptotheci n, *J. Drug Targeting*, 12(6) 373-84 (2004).
43) P. Opanasopit, M. Yokoyama, M.Watanabe, K. Kawano, Y. Maitani, T. Okano, Block copolymer design f or camptothecin incorporation into polymeric micelles for passive tumor targeting, *Pharm. Res.*, 21 (11) 2003-2010 (2004).

Degradation Rate of Lyophilized Insulin, Exhibiting an Apparent Arrhenius Behavior around Glass Transition Temperature Regardless of Significant Contribution of Molecular Mobility

SUMIE YOSHIOKA, TAMAKI MIYAZAKI, YUKIO ASO

National Institute of Health Sciences, 1-18-1 Kamiyoga, Setagaya-ku, Tokyo 158-8501, Japan

Received 3 February 2006; revised 13 April 2006; accepted 10 May 2006

Published online 4 August 2006 in Wiley InterScience (www.interscience.wiley.com). DOI 10.1002/jps.20689

ABSTRACT: The relative influences of chemical activation energy and molecular mobility in determining chemical reactivity were evaluated for insulin lyophilized with α,β-poly(*N*-hydroxyethyl)-L-aspartamide (PHEA), and compared with that for insulin lyophilized with trehalose, which had been found to have the ability to decrease the molecular mobility of insulin at low humidity. The ratio of the observed rate constant k_{obs} to the chemical activation energy-controlled rate constant k_{act} (k_{obs}/k_{act}) at glass transition temperature (T_g) was estimated to be approximately 0.6 and 0.8 at 6% RH and 12% RH, respectively, indicating that the degradation rate is significantly affected by molecular mobility at lower humidity conditions. However, these k_{obs}/k_{act} values at T_g were larger than those for the insulin-trehalose system, and changes in the temperature-dependent slope around T_g were less obvious than those for the insulin-trehalose system. Thus, the contribution of molecular mobility to the degradation rate in the insulin-PHEA system appeared to be less intense than that in the insulin-trehalose system. The subtle change in the temperature-dependent slope around T_g observed in the insulin-PHEA system brought about a significant bias in shelf-life estimation when the reaction rate was extrapolated from temperatures above T_g according to the Arrhenius equation.
 J Pharm Sci 95:2684–2691, 2006
Keywords: solid state stability; glass transition; lyophilization; amorphous; shelf life; molecular mobility

INTRODUCTION

It is generally thought that the chemical reactivity of amorphous pharmaceutical formulations is controlled not only by chemical activation energy but also by molecular mobility.[1,2] An understanding of which factor is the dominant influence on the chemical reactivity of a given system (via quantitative assessment of the relative significance of chemical activation energy and molecular mobility as a determinant of chemical reaction rate) would provide some practical benefit for stabilization strategy during formulation development. Furthermore, such an assessment would allow us to examine the feasibility of extrapolating the reaction rate obtained under accelerated conditions in order to determine the reaction rate at lower temperatures.

For a chemical reaction that involves a diffusive step for the reactants, as for a bimolecular reaction, a decrease in molecular mobility results in a decrease in reaction rate. The degree of reduction in degradation rate caused by reduced molecular mobility can be evaluated using the indicator k_{obs}/k_{act} (the ratio of the observed rate

Correspondence to: Sumie Yoshioka (Telephone: 81-3-3700-8547; Fax: 81-3-3707-6950; E-mail: yoshioka@nihs.go.jp)

Journal of Pharmaceutical Sciences, Vol. 95, 2684–2691 (2006)

constant k_{obs} to the chemical activation energy-controlled rate constant k_{act}, the latter being the rate constant in a system in which the reactants have sufficiently high molecular mobility). In previous studies, we determined k_{obs}/k_{act} values for insulin degradation via formation of the cyclic anhydride intermediate in lyophilized formulations containing various excipients, and demonstrated that k_{obs} was dominantly controlled by chemical activation energy and was unaffected by molecular mobility for insulin lyophilized with poly(vinylpyrrolidone)[3,4] or dextran[5] under a wide range of conditions of temperature and humidity. In contrast, k_{obs} for insulin lyophilized with trehalose was substantially affected by molecular mobility under conditions of lower humidity[3]; it was found that β-relaxation of the insulin molecule, as determined by NMR relaxation time, was inhibited by addition of trehalose, resulting in a decrease in the degradation rate.[5]

In this study, the effect of excipients on the relative influences of molecular mobility and chemical activation energy on insulin degradation rate was further examined using insulin lyophilized with α,β-poly(*N*-hydroxyethyl)-L-aspartamide (PHEA), which is expected to inhibit β-relaxation of the insulin molecule through hydrogen-bonding in a manner similar to trehalose. k_{obs}/k_{act}, a parameter representing the degree of reduction in degradation rate caused by reduced molecular mobility, was calculated for the insulin-PHEA system, and assessed for the reliability by simulation studies. In addition, the practical meaning of the estimated k_{obs}/k_{act} was considered in terms of shelf-life estimates which may be biased by ignoring the effect of molecular mobility.

BACKGROUND

Eq. 1 was proposed to calculate the degree of reduction in degradation rate caused by reduced molecular mobility in amorphous solids (k_{obs}/k_{act}).[3]

$$k_{obs} = k_{act}\left(\frac{\alpha T\left(\frac{1}{\tau}\right)^{\xi}}{k_{act} + \alpha T\left(\frac{1}{\tau}\right)^{\xi}}\right) \quad (1)$$

Eq. 1 is derived from the Collins and Kimball (CK) equation,[6,7] which describes k_{obs} for bimolecular reactions as a function of k_{act} and the diffusion-controlled rate represented using the diffusion coefficient. The CK equation was modified by describing the diffusion-controlled rate in terms of structural relaxation time (τ) instead of the diffusion coefficient, assuming that the diffusion coefficient is inversely correlated to τ. α is a constant that represents the correlation between τ and the diffusion-controlled rate, and ξ is a constant that represents the degree of coupling between τ and the diffusion coefficient.[8] τ in Eq. 1 can be calculated from T_g and fragility parameter (m) using the Vogel–Tammann–Fulcher (VTF) and Adam–Gibbs–Vogel (AGV) equations above and below T_g, respectively, as described previously.[3] k_{act} in Eq. 1 is described as follows:

$$k_{act} = A\exp\left(\frac{-E_a}{RT}\right) \quad (2)$$

where A, E_a, and R are the frequency factor, activation energy, and gas constant. For a first-order reaction, the time required for 10% degradation (t_{90}) can be calculated from k_{obs} as:

$$t_{90} = -\ln(0.9)/k_{obs}$$

The previous article briefly described how the contribution of molecular mobility to chemical reactivity is affected by E_a and α,[3] but it was not easily understandable what combination of E_a and α yields a chemical reaction exhibiting a greater contribution of molecular mobility to the reactivity. Therefore, comprehensible figures are presented for a better understanding of the effects of E_a and α on the values of k_{obs}/k_{act}, which were calculated using a model system with T_g of 70°C, m of 50 and A of 1×10^{14}/s.

As shown in Figure 1, k_{obs}/k_{act} and t_{90} at T_g largely depend on E_a and α. When E_a increases beyond the value at which k_{obs}/k_{act} is equal to 0.5 (i.e., k_{obs} is reduced to half of k_{act} due to reduced mobility), k_{obs}/k_{act} gradually approaches unity, indicating a decrease in the effect of molecular mobility and an increase in the effect of E_a. Thus, t_{90} at T_g ($t_{90(Tg)}$) becomes dependent only on E_a, and increases with increasing E_a. In contrast, when E_a decreases below the value at which k_{obs}/k_{act} is equal to 0.5, k_{obs}/k_{act} gradually approaches zero, indicating an increase in the effect of molecular mobility and a decrease in the effect of E_a. Thus, t_{90} becomes independent of E_a, and is controlled only by molecular mobility. The E_a value at which k_{obs}/k_{act} is equal to 0.5 increases with decreasing α.

As shown in Figure 2, when α increases beyond the value at which k_{obs}/k_{act} is equal to 0.5, k_{obs}/k_{act} gradually approaches unity, indicating a decrease in the effect of molecular mobility. Thus, $t_{90(Tg)}$ becomes independent of α, and is controlled only by

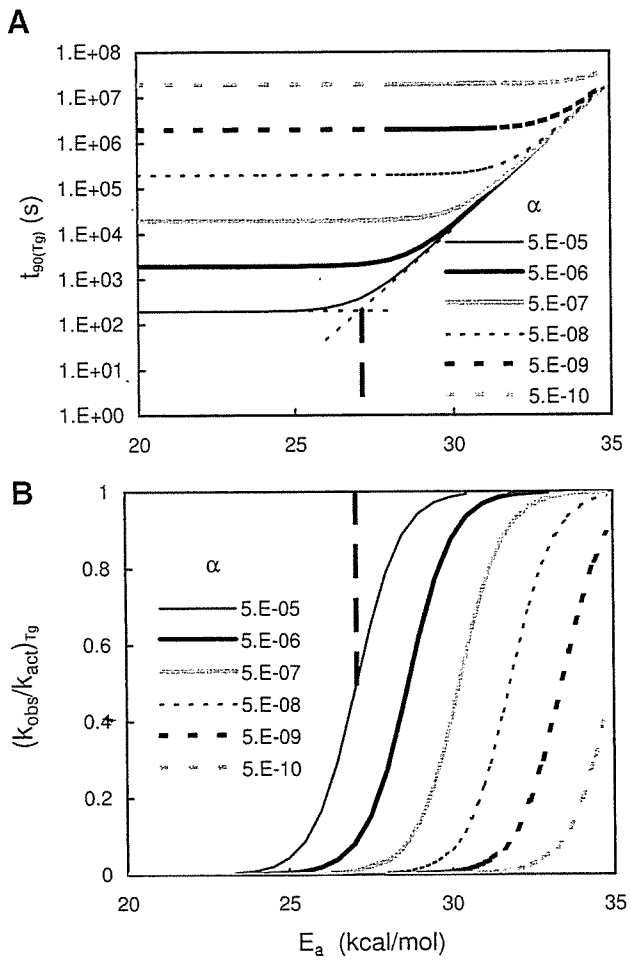

Figure 1. Effect of E_a on the values of t_{90} at T_g (A) and k_{obs}/k_{act} at T_g (B). T_g: 70°C; m:50; A:1 × 10^{14}/s.

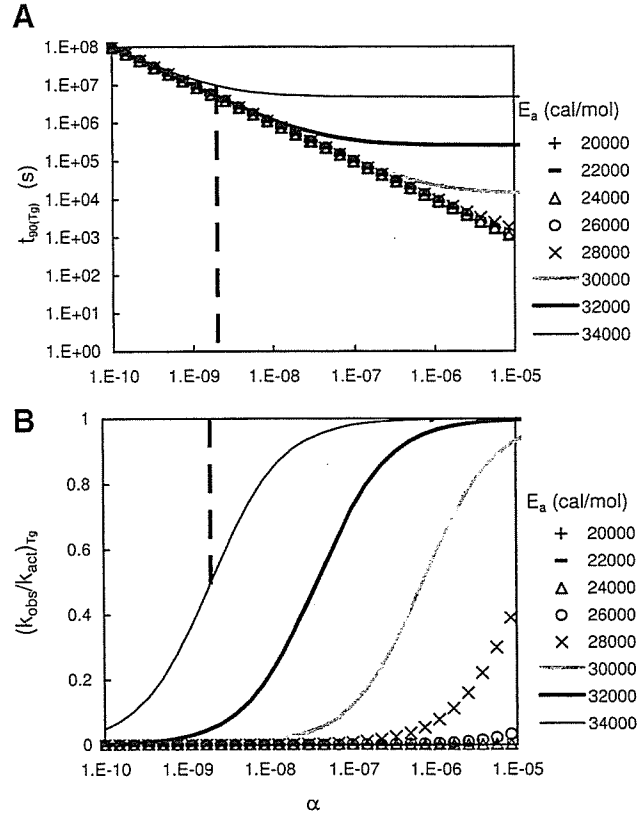

Figure 2. Effect of α on the values of t_{90} at T_g (A) and k_{obs}/k_{act} at T_g (B). T_g: 70°C; m:50; A:1 × 10^{14}/s.

E_a. In contrast, when α decreases below the value at which k_{obs}/k_{act} is equal to 0.5, k_{obs}/k_{act} gradually approaches zero, indicating an increase in the effect of molecular mobility. Thus, $t_{90(Tg)}$ becomes independent of E_a, and increases with decreasing α. The α value at which k_{obs}/k_{act} is equal to 0.5 increases with decreasing E_a.

Some equations for describing the relationship between molecular mobility and chemical reactivity in amorphous solids have been described in the literature. Pikal[1] presented Eq. 3 to describe the temperature dependence of the degradation rate constant for a diffusion-controlled reaction, using a coupling constant (g), the strength parameter for structural relaxation (D), and the temperature at which the configurational entropy is zero (T_0):

$$k = A_k \exp\left(-\frac{gDT_0}{T-(T/T_f)T_0}\right) \quad (3)$$

where A_k is a pre-exponential constant that depends on the details of the degradation mechanism. A_k would be expected to decrease as the number of diffusional jumps needed to complete a reaction increases. Eq. 3 may be written in the form $k = A_k(\tau_0/\tau)^g$ using a value for structural relaxation time (τ). On the other hand, Eq. 1 may be written in the form $k_{obs} = \alpha T/\tau^{\xi}$ when the reaction is diffusion-controlled such that the rate is independent of E_a. Therefore, the terms αT and ξ in Eq. 1 correspond to $A_k\tau_0^g$ and g, respectively, in Eq. 3. Therefore, a decrease in α, a parameter representing the degree of inverse correlation between τ and the diffusion-controlled rate, may correspond to an increase in the number of jumps required for the reaction to proceed, leading to a greater degree of reduction in degradation rate due to reduced molecular mobility.

Craig et al.[7] presented Eq. 4 to describe the relationship between degradation rate and viscosity (η) for diffusion-controlled bimolecular reaction:

$$k = 8RT/3\eta \quad (4)$$

DOI 10.1002/jps

where R is the gas constant. Eq. 4 may be written in the form $k = 8RT\tau_{Tg}/3\eta_{Tg}\tau$, using values of τ_{Tg} and η_{Tg} (τ and η at T_g, respectively) as well as τ. Therefore, the term α in Eq. 1 corresponds to $8R\tau_{Tg}/3\eta_{Tg}$.

EXPERIMENTAL

Materials

Human zinc insulin was purchased from Eli Lilly & Co (Humulin® RU-100. PHEA was prepared via polysuccinimide by polycondensation of aspartic acid as reported.[9]

Lyophilization of Insulin

Lyophilization was carried out in a similar manner as reported previously.[3] Human zinc insulin was converted into the zinc-free neutral form by dialysis. PHEA was added to the solution to make a 5 mg/mL of PHEA solution and pH was adjusted to 4.0. The ratio of insulin to PHEA was 1:1.5 w/w. Four hundred microliters of the solution were frozen in a polypropylene sample tube (10 mm diameter), and then dried at a vacuum level below 5 Pa for 23.5 h in a lyophilizer (Freezevac C-1, Tozai Tsusho Co., Tokyo, Japan). The shelf temperature was between −35 and −30°C for the first 1 h, 20°C for the subsequent 19 h, and 30°C for the last 3.5 h.

Lyophilized samples were stored at 15°C for 24 h in a desiccator with a saturated solution of LiBr H_2O (6% relative humidity (RH)), LiCl (12% RH), potassium acetate (23% RH), K_2CO_3 $2H_2O$(43% RH), or NaBr $2H_2O$ (60% RH) to obtain samples with various T_g values.

Determination of T_g by Differential Scanning Calorimetry (DSC)

Modulated temperature DSC experiments were performed using a commercial system (2920; TA Instruments, Newcastle, DE, USA) attached to a refrigerated cooling accessory. The conditions were as follows: modulation period of 100 s, a modulation amplitude of ±0.5°C, and an underlying heating rate of 1°C/min. Samples were put in a hermetic pan. Temperature calibration was performed using indium. The samples, pre-equilibrated at 6% RH, 12% RH, 23% RH, 43% RH, and 60% RH, exhibited a T_g value of 70°C, 60°C, 36°C, 17°C, and −17°C, respectively.

Measurement of Insulin Degradation

Lyophilized samples with various T_g values in tubes with a tight screw-cap were stored at a constant temperature (40–95°C), removed at various times, and stored in liquid nitrogen until assayed. Samples were dissolved in 1.5 mL of 0.01 M $(NH_4)_2SO_4$ (pH 2.2, adjusted with concentrated H_2SO_4) and each 20 μL aliquot of the solution (insulin concentration was 0.9 mg/mL) was subjected to reverse phase HPLC, as reported previously.[3] The column used was Inertsil WP-300 (C8, 4.6 mm × 250 mm, GL Science, Inc., Tokyo, Japan) maintained at 35°C. Elutions were performed using a mixture of 0.01 M $(NH_4)_2SO_4$ (pH 2.2) and acetonitrile solution of 0.07%(v/v) trifluoroacetic acid (72.5:27.5) for 1 min. The ratio of the acetonitrile solution increased linearly from 27.5% to 30% in 15 min, 30% to 35% in 22 min. The detection wavelength was 214 nm.

Decreases in intact insulin with storage time was due to the formation of the cyclic anhydride intermediate followed by formation of A21-desamido insulin and insulin dimer, as previously reported for insulin degradation in lyophilized formulations containing trehalose, poly(vinylpyrrolidone), and dextran.[3–5]

RESULTS AND DISCUSSION

Figure 3 shows the degradation time courses for insulin lyophilized with PHEA at 6% RH. Similar time courses were obtained at 12% RH, 23% RH, 43% RH, and 60% RH. The initial stage of

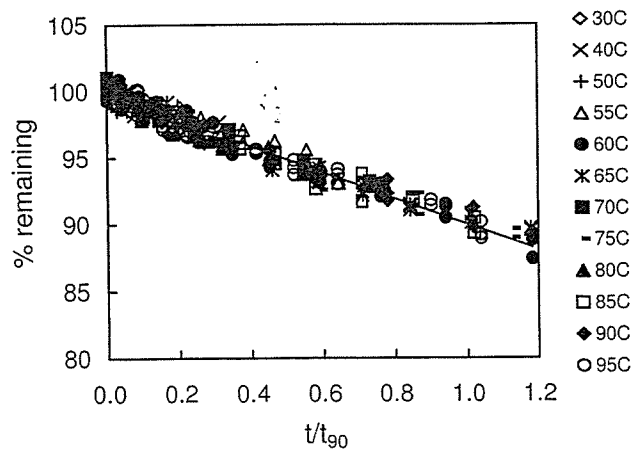

Figure 3. Degradation time courses of insulin lyophilized with PHEA at 6% RH and various temperatures. Solid line represents the theoretical line calculated according to the first-order kinetics.

degradation was describable with first-order kinetics under all the temperature and humidity conditions studied. The solid line in Figure 3 represents the theoretical time course of first-order kinetics.

The obtained k_{obs} was used to calculate t_{90}, and the temperature dependence of t_{90} is shown in Figure 4. Regression analysis according to Eq. 1 was performed assuming that formation of the cyclic anhydride intermediate involves a diffusive step for the reaction site (i.e., molecular mobility required for the intermediate formation is related to diffusion coefficient). The values of A and ξ were assumed to be 10^{14}/s and 0.75, respectively. ξ of 0.75 has been obtained for various organic glasses.[10] The value of τ was calculated according to the VTF and AGV equations above and below T_g, respectively, using T_g values measured by DSC and m of 50 (m value estimated for insulin lyophilized with trehalose in the previous study).[3] Lines in Figure 4 represent regression curves for the t_{90} obtained under various humidity conditions. The values of α and E_a were estimated to be 5×10^{-8} deg^{-1} and 32 kcal/mol, respectively, for degradation at 6% RH. Although the temperature dependence of t_{90} appeared to be linear under all humidity conditions investigated, regression analysis according to Eq. 1 provided k_{obs}/k_{act} values at T_g of approximately 0.6 and 0.8 at 6% RH and 12% RH, respectively, as shown in Figure 5. This finding indicates that the degradation rate is significantly affected by molecular mobility at lower humidity conditions.

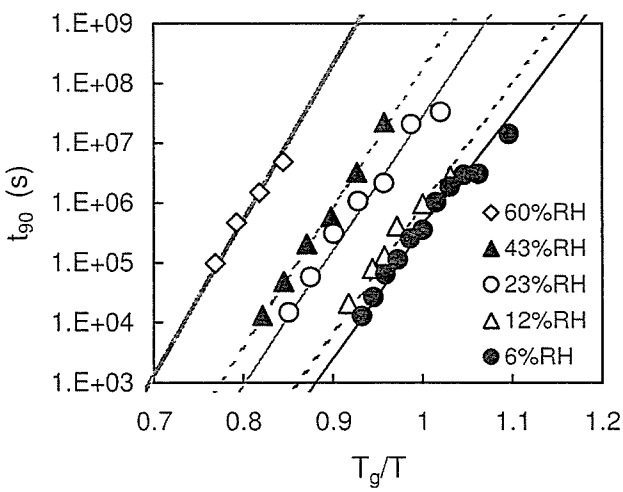

Figure 4. Temperature dependence of t_{90} calculated from apparent first-order rate constant for insulin degradation. Solid lines represent the regression lines obtained according to Eq. 1.

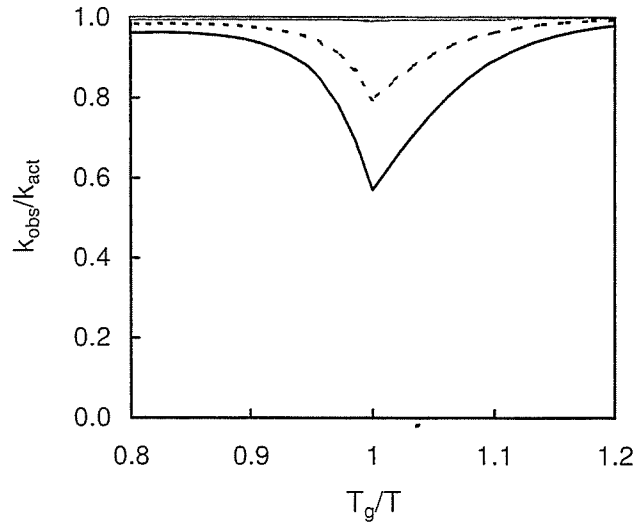

Figure 5. Temperature dependence of k_{obs}/k_{act}, a parameter representing the degree of reduction in degradation rate caused by reduced molecular mobility, obtained at 6% RH (solid line) and 12% RH (dotted line).

As previously reported,[3–5] insulin lyophilized with trehalose exhibited a k_{obs}/k_{act} value at T_g of approximately 0.05, and insulin lyophilized with PVP or dextran exhibited a k_{obs}/k_{act} value at T_g of unity for degradation at 12% RH. Therefore, the effect of molecular mobility on degradation rate in the insulin-PHEA system appeared to be less intense than that in the insulin-trehalose system, but not negligible compared to the insulin-PVP and insulin-dextran systems.

The reliability of the values of α and E_a estimated for insulin degradation at 6% RH in the insulin-PHEA system (5×10^{-8} deg^{-1} and 32 kcal/mol, respectively) was examined from changes in the temperature dependence of t_{90} accompanied by changes in α and E_a. Figure 6A shows the effect of changes in E_a on the temperature dependence of t_{90}. The temperature dependence of t_{90} obtained by curve fitting of the observed degradation data to Eq. 1 is represented by the bold solid line (E_a: 32 kcal/mol), along with that of the values of t_{90} derived from k_{act} ($t_{90(act)}$), indicated by symbol +. Although the difference between t_{90} and $t_{90(act)}$ was slight even at T_g, the value of k_{obs}/k_{act} was approximately 0.6 at T_g (Fig. 6B). When E_a increases by 2 kcal/mol (E_a: 34 kcal/mol), the difference between t_{90} (solid line) and $t_{90(act)}$ (circle symbol) becomes unnoticeable, with a k_{obs}/k_{act} value greater than 0.9. Conversely, when E_a decreases by 2 kcal/mol (E_a: 30 kcal/mol), the difference between t_{90} (dotted line) and $t_{90(act)}$ (star symbol) becomes substantial, such that t_{90} is

 DOI 10.1002/jps

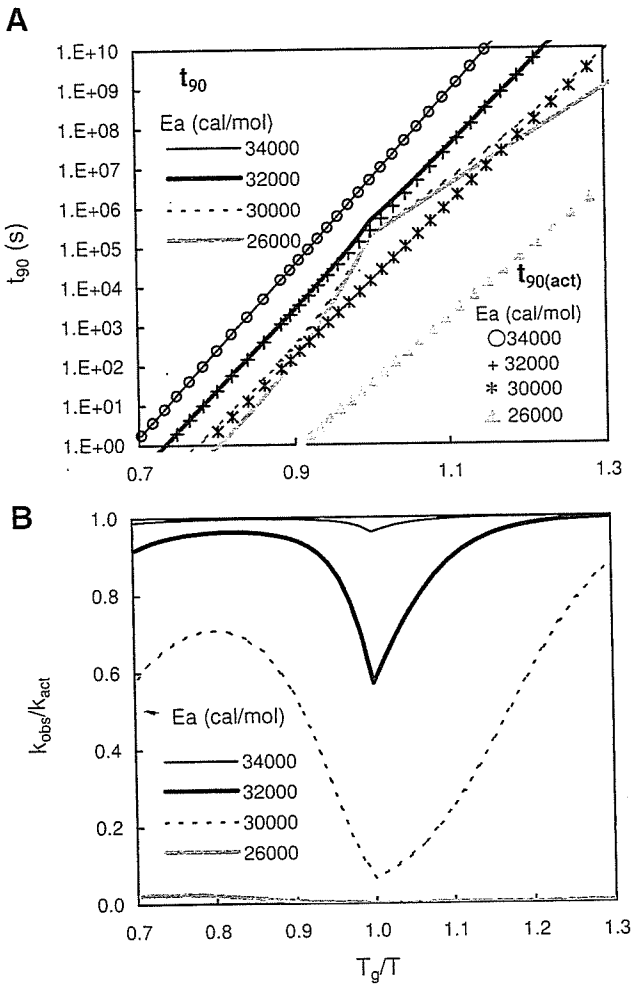

Figure 6. Divergence of temperature dependence for t_{90} and $t_{90(act)}$ (A), and for k_{obs}/k_{act} (B) from that obtained at 6% RH, associated with changes in E_a. α:5×10^{-8}.

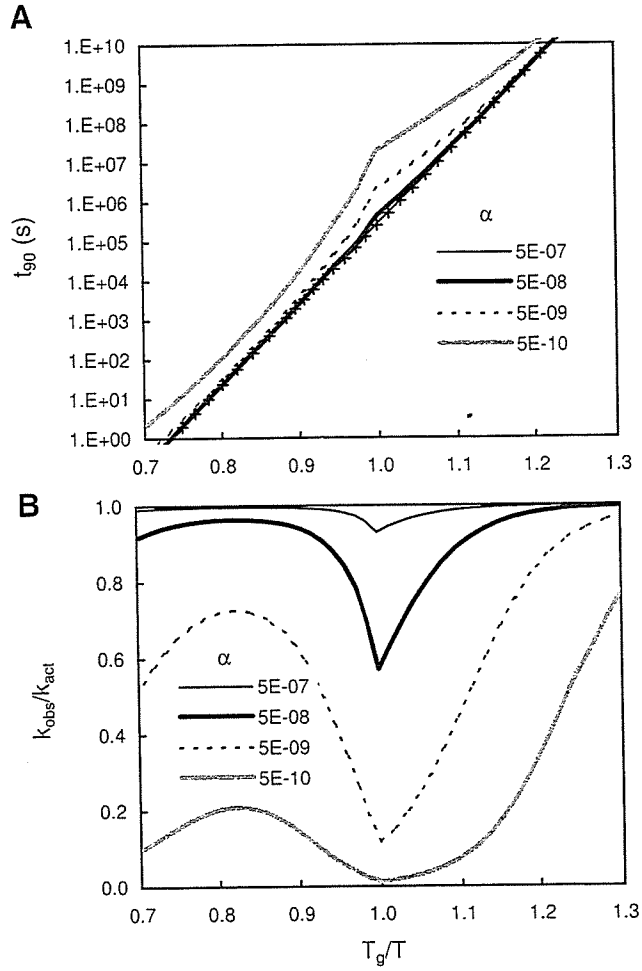

Figure 7. Divergence of temperature dependence for t_{90} (A) and for k_{obs}/k_{act} (B) from that obtained at 6% RH, associated with changes in α. E_a:32 kcal/mol.

affected by E_a only at temperatures well below or well above the T_g, with a k_{obs}/k_{act} value at T_g of less than 0.1. A further decrease in E_a (E_a: 26 kcal/mol) causes a further decrease in $t_{90(act)}$, but no significant change in t_{90} around T_g. Figure 7 shows changes in the temperature dependence of t_{90} accompanied by changes in α. When α becomes about one order of magnitude less than the estimated α value, the degree of reduction in degradation rate caused by reduced molecular mobility becomes obvious. Thus, the estimated values of α and E_a appeared to be reliable with errors of one order of magnitude and 2 kcal/mol of magnitude, respectively. The ξ value of 0.75 used in regression analysis was validated in terms of changes in the temperature dependence of t_{90} with varying ξ. With ξ of unity, as shown in Figure 8, a change in the temperature-dependent slope around T_g is more obvious than that with ξ of 0.75, and diverged from the observed data of t_{90}.

For an understanding of the practical implication of the k_{obs}/k_{act} (degree of reduction in degradation rate caused by reduced molecular mobility) of 0.6 obtained at 6% RH, t_{90} at 25°C ($t_{90(25C)}$) was estimated from only the degradation data obtained at temperatures above T_g, using the Arrhenius equation, with the subtle change in temperature-dependent slope ignored. Table 1 compares $t_{90(25C)}$ obtained according to the Arrhenius equation, along with the theoretical $t_{90(25C)}$ obtained according to Eq. 1. The estimates of t_{90} at 25°C were greater than the theoretical values by factors of 2.7 and 1.3 at 6% RH and 12% RH, respectively. To gain a further insight into the practical meaning of the k_{obs}/k_{act} value, bias in the $t_{90(25C)}$ estimate obtained by neglecting the effect of molecular mobility was calculated as a function of k_{obs}/k_{act} for

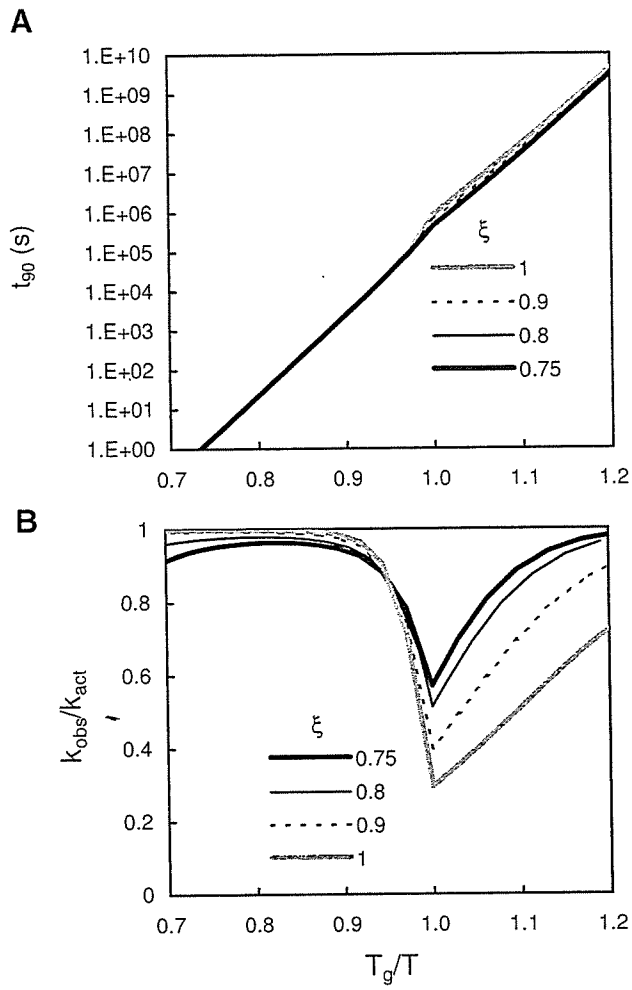

Figure 8. Divergence of temperature dependence for t_{90} (A) and for k_{obs}/k_{act} (B) from that obtained at 6% RH, associated with changes in ξ. E_a:32 kcal/mol; α:5×10^{-8}.

a degradation model with an E_a value corresponding to a t_{90} of 1 year for reaction-controlled degradation, and the results are shown in Figure 9. The bias of the $t_{90(25C)}$ estimate increased as k_{obs}/k_{act} decreased (i.e., as the effect of molecular mobility increased), with a $t_{90(25C)}$ estimate of approximately 3 years at a k_{obs}/k_{act} of 0.6. These findings indicate that even a subtle change in the temperature dependence of t_{90} around T_g, as

Table 1. Effect of Ignored Contribution of Molecular Mobility on the t_{90} Estimates at 25°C

Humidity (%RH)	$t_{90(Eq.\ 1)}$ (Year)	$t_{90(Arrh)}$ (Year)	$t_{90(Arrh)}/t_{90(Eq.\ 1)}$
6	10.3	27.6	2.7
12	7.2	9.7	1.3

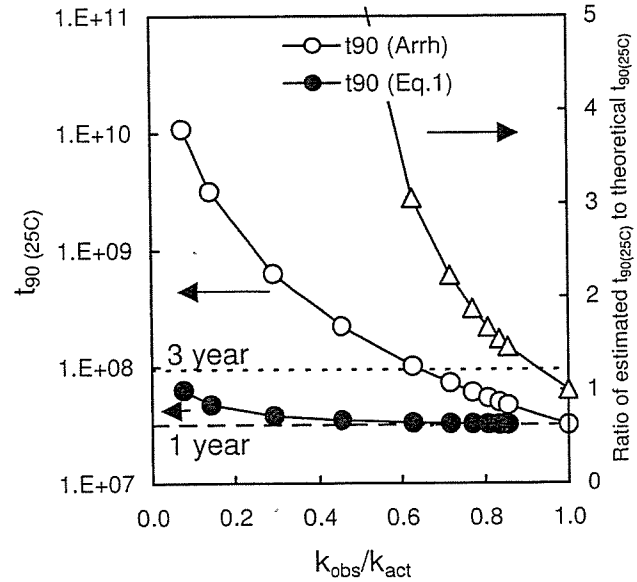

Figure 9. Effect of k_{obs}/k_{act} on $t_{90(25C)}$ estimated by neglecting the effect of molecular mobility. Triangle represents the ratio of $t_{90(25C)}$ estimate to the theoretical $t_{90(25C)}$.

shown for degradation at 6% RH (Fig. 4), can lead to significantly biased shelf-life prediction.

CONCLUSION

Chemical degradation of insulin lyophilized with PHEA under low humidity conditions exhibited a temperature dependence with a less obvious change around T_g than that of insulin lyophilized with trehalose. The contribution of molecular mobility to the degradation rate was found to be less than that for the insulin-trehalose system. However, the subtle change in slope resulted in a significant bias in shelf-life estimation when the reaction rate was extrapolated from temperatures above T_g according to the Arrhenius equation.

REFERENCES

1. Pikal MJ. 2004. Mechanisms of protein stabilization during freeze-drying and storage: The relative importance of thermodynamic stabilization and glassy state relaxation dynamics. In: Freeze-drying/lyophilization of pharmaceutical and biological products. 2nd ed. New York: Marcel Dekker, Inc., pp 63–107.
2. Parker R, Gunning YM, Lalloue B, Noel TR, Ring SG. 2002. Glassy state dynamics, its significance for

DOI 10.1002/jps